Biodegradable Thermoplastic Polyurethanes Incorporating Polyhedral Oligosilsesquioxane

Pamela T. Knight,[†,‡] Kyung Min Lee,[†] Haihu Qin,[†] and Patrick T. Mather*[,‡,§]

Department of Macromolecular Science and Engineering, Case Western Reserve University, 2100 Adelbert Road, Cleveland, Ohio 44106, Syracuse Biomaterials Institute, and Department of Biomedical and Chemical Engineering, Syracuse University, Syracuse, New York 13244

Received May 4, 2008; Revised Manuscript Received June 23, 2008

A new hybrid thermoplastic polyurethane (TPU) system that incorporates an organic, biodegradable poly(D,L-lactide) soft block with a hard block bearing the inorganic polyhedral oligosilsesquioxane (POSS) moiety is introduced and studied. Changes in the polyol composition made through variation of the hydrophilic initiator molecular weight show direct control of the final transition temperatures. Incorporating POSS into the hard segments allows for excellent elasticity above T_g, as evidenced with dynamic mechanical analysis, not seen in most other biodegradable materials. This elasticity is attributed to physical cross-links formed in the hard block through POSS crystallization, as revealed with wide-angle X-ray diffraction. Increasing the POSS incorporation level in the TPU hard block was observed to increase crystallinity and also the rigidity of the material. The highest incorporation, using a statistical average of three POSS units per hard block, demonstrated one-way shape memory with excellent shape fixing capabilities. In vitro degradation of this sample was also investigated during a two month period. Moderate water uptake and dramatic molecular weight decrease were immediately observed although large mass loss (~20 wt %) was not observed until the two month time point.

Introduction

The degree of control over both the architecture and composition of polymeric biomaterials has increased dramatically over the past few years, affording a wide range of materials for use in drug delivery, gene therapy, tissue engineering, bone scaffolds, and even organ replacement. For applications employing degradable components, aliphatic polyesters have been at the forefront due to their simple breakdown through hydrolysis into biocompatible components.[1−3] Among these polymers, the most prominent include poly(lactide), poly(glycolide), copolymers of lactide and glycolide, and poly(caprolactone). Poly(lactide)-based polymers (hereafter, "PLA") have shown particular potential, especially since they can be made from natural, renewable resources and numerous medical devices utilizing PLA have been approved by the FDA since the 1970s. Lactide, derived from the dimerization of lactic acid, contains two stereocenters and can therefore be polymerized into homopolymers made from the pure D (PDLA) or L (PLLA) enantiomer, or synthesized into a copolymer by using both. Pure racemic copolymerization of alternating D- and L-configured repeat units (PDLLA) creates a completely amorphous, fast degrading polymer. On the other hand, once a significant block of pure enantiomer has been achieved, both the D and L repeat units can crystallize and even form complexes with each other, resulting in slower degradation. Current research has focused on the PLLA homopolymer since the L-enantiomer is more commonly found in vivo and its homopolymer provides some of the thermal and mechanical properties necessary to undergo implantation into a human body. In order to achieve a wide range of properties further than what PLA can provide alone, lactide has also been combined with other monomers and polymers such as poly(ethylene glycol) for increased hydrophilicity[4−6] and ϵ-caprolactone for increased flexibility.[7−9] Alternatively, various architectures, aside from linear chains, have been investigated including cross-linked networks, star polymers, and stereocomplexes (as mentioned above).

Another approach to the modification of degradable polymers, such as PLA, has been the copolymerization of polyesters with other, more rigid molecules to formulate blocky thermoplastic polyurethanes (TPUs).[10−13] In such compositions, the degradable feature of the polyester component (soft block) is afforded desirable structural characteristics associated with engineering thermoplastics, including modulus increase, ductility, and thermal stability. This is achieved through the block-wise incorporation of reinforcing elements in the form of self-assembling, higher melting hard blocks distributed uniformly throughout the material with a volume fraction prescribed in the TPU formulation by the ratio of chain extender (hard block forming) to biodegradable polyol. These types of biomaterials have become important when a combination of robust mechanical features and controlled degradation are needed.

One mechanical property of thermoplastic polyurethanes being exploited by the present work is the ability to perform shape memory cycles, i.e. able to fix a temporary shape and then recover to the original shape by cooling/heating through a thermal transition. Shape memory requires elevated temperature elasticity, provided through either physical or chemical cross-links, as well as a percolating phase capable of reversibly "fixing" an applied deformation.[14,15] In the case of a biodegradable thermoplastic, the physical cross-links employed should be tuned to be strong enough for elasticity, but not so strong as to unfavorably alter degradation. Our method for satisfying these requirements will be a hybrid approach utilizing POSS crystallization, and is discussed in detail below. For the percolating network, it has been found that polyol molecular weights in the 2−4 kg/mol range are not sufficient to allow large strain

* To whom correspondence should be addressed. E-mail: ptmather@syr.edu.
[†] Case Western Reserve University.
[‡] Syracuse Biomaterials Institute.
[§] Department of Biomedical and Chemical Engineering.

10.1021/bm8004935 CCC: $40.75
Published on Web 08/13/2008

(>100%) elastic deformations. Due to this constraint, our work has settled in on a polyol molecular weight in the 12 kg/mol range. For controlled shape memory activation in the narrow window of 37 °C < T_{crit} < 50 °C (physiological to tissue-burning) precise control over the shape memory fixing phase transition temperature is needed and we achieve this herein with unique yet simple polyol compositions. Even moisture activation, without excessive swelling, will be possible.

Combining organic and inorganic materials into hybrid biomaterials is an active area of research in which the goal is to achieve properties that combine desirable features of polymers and ceramics, but maintaining biocompatibility and, in some cases, biodegradability.[16] Aside from simple filler incorporation via compounding, the most common approach to achieve hybrid biomaterials is the in situ hydrolysis and condensation of the inorganic oxide, usually silica from tetraethylorthosilicate (TEOS), within a relatively polar polymeric host. A significant challenge of this approach, however, is the lack of molecular and microstructural control now possible with synthetic polymers. In particular, high variability exists in the degree of condensation to silica (SiO_2), particle size, and spatial distribution in TEOS-based hybrid materials[17−19] even when adopting the biomimetic approach of protein-based biomineralization.[20−23] An alternative approach to hybrid materials synthesis that addresses these challenges has been the use of the precondensed polyhedral oligosilsesquioxane (POSS*)[24] moiety, functionalized for polymerization or grafting.[25−38] (*POSS is a registered trademark of Hybrid Plastics, Inc.) These large hybrid molecules have the unique feature of containing both an inorganic silicon−oxygen cage (Si_8O_{12}) and up to eight compatibilizing organic groups pendant to each silicon corner of the cage. Typically, one or more of those groups contains the appropriate functionality to incorporate POSS into a variety of compositions, including thermoplastics[39−42] and thermosets[30,43−46] through either copolymerization or blending. Despite the extensive reports on POSS inclusion into polymers, comparatively little research focused on biomaterials featuring POSS incorporation.[24,47]

Past research has found a difference in self-assembly of POSS moieties within polymeric hosts, depending on the macromolecular architecture of POSS incorporation. In random POSS-copolymers, the POSS moieties have been found to aggregate into noncrystalline, nanometer-dimensioned (10−100 nm) domains.[33,34,48,49] In contrast, architectural localization of POSS to the chain ends (telechelics[29,50−52]) or to blocks within block copolymers[28,31,53] or within multiblock copolymers, specifically polyurethanes with POSS as the hard block,[47,54−57] has been found to allow long-range ordering of the POSS groups in the form of crystallization. This inherent aggregation or crystallization of POSS groups in the aforementioned morphologies allows for the formation of physically cross-linked networks with robust properties. The present work illustrates a unique combination of thermoplastic properties with biomedical attributes to introduce a hybrid polyurethane that is rendered mechanically stable (elastic) above the glass transition temperature through POSS hard block crystallization, but also biodegradable through the PEG-modified poly(lactide) soft blocks. Preliminary results on this family of materials were first established in 2006[41,58] along with patents covering the compositions of matter and medical applications,[59,60] while the present manuscript represents our first in-depth study on the materials. As will be made clear, numerous variations in composition and architecture are possible for the present POSS-based TPUs, including polyol composition (esp. hydrophobicity), molecular weight, initiator and diisocyanate composition, and hard block (POSS) to soft block ratio. We focus here on two particular synthetic variables found to be particularly effective in manipulating physical properties; namely, polyol initiation with PEG chains of varying molecular weight and POSS/polyol ratio. Focus is placed upon the associated structure−property relationships with an eye toward intended medical applications.

Experimental Section

Materials and Methods. 3,6-Dimethyl-1,4-dioxane-2,5-dione (lactide monomer, **LA**) was purchased from Aldrich and purified by recrystallization in ethyl acetate (40 g/200 mL) to give white, flaky crystals. The lysine-derived diisocyanate, methyl 2,6-diisocyanatohexanoate (**LDI**), a liquid, was purchased from Kyowa Hakko Chemical Company, purified of any moisture-reacted side products by vacuum distillation, and stored under nitrogen prior to use. Organometallic catalysts used for polyol and TPU synthesis included tin 2-ethylhexanoate (stannous octanoate) and dibutyltin dilaurate, respectively, and these were purchased from Aldrich each with a purity of 95%. Each catalyst was used as received. Poly(ethylene glycol)s with varying molecular weight of 0.6, 1.0, 2.0, and 4.0 kg/mol (referred to as **P(0.6k)**, **P(1k)**, **P(2k)**, **P(4k)**) were purchased from Alfa Aesar and used without further purification. 2,2,4-trimethyl-1,3-pentane (TMP) POSS diol (R-group = ^{t}Bu), hereafter "POSS diol" was purchased from Hybrid Plastics, Inc. as a pure (99.5%) crystalline powder and used as received. All reactants were dried overnight in vacuo at 50 °C before running either the polyol or polyurethane reaction. Toluene, tetrahydrofuran (THF), hexanes, and ethyl acetate were purchased from Fisher, with the toluene dried by refluxing over CaH_2 for several hours before being dispensed for immediate use. Buffer used for the degradation study was made from phosphate buffered saline (PBS) buffer packets (Sigma) containing 0.05% Tween-20 and having a final pH of 7.4 and concentration of 0.01 M when combined with one liter of deionized water.

Structural compositions of the final products were analyzed using liquid phase ^{1}H NMR with a Varian Inova spectrometer operating at 600 MHz. Samples were made from $CDCl_3$ solutions and run at room temperature.

Gel permeation chromatography (GPC) was conducted using a Waters Isocratic HPLC system equipped with a temperature controlled differential refractometer (Waters 2414, held at 35 °C). Multiangle laser light scattering was also employed (Wyatt miniDAWN) using three angles (45°, 90°, 135°) for in-line absolute molecular weight determination. THF solutions (~2 mg/mL) were passed through a 0.2 μm PTFE filter prior to injection. The GPC was operated at a flow rate of 1 mL/min and featured a series of three (3) columns of cross-linked polystyrene beads. The columns were 5 cm (first) and 30 cm long (second and third) ResiPore columns (Polymer Laboratories, Inc.), consecutively, each packed with 3 μm particles designed for separations of polymers with molecular weight less than 400 kg/mol.

Differential scanning calorimetry (DSC) was used to determine the phase behavior and thermal transitions of polyols and TPUs, alike, and was performed using a TA Instruments Q100 apparatus under flowing nitrogen gas. Samples were made by encapsulating approximately 3 to 5 mg of polymer in a TA aluminum pan. The heating and cooling rate for each sample was 10 °C/min, unless otherwise mentioned, and the heat flow traces shown are from second heating runs, thus having erased all thermal history (held for five minutes at 80 °C for polyols and 160 °C for TPUs). Glass transition temperatures (T_g) were taken as the midpoint of the stepwise decrease of the heat flow trace (stepwise increase in heat capacity) observed during heating. Melting points (T_m) were taken as the temperatures corresponding to the valley (most negative value) of the endothermic transition during the second heat, with heats-of-fusion (ΔH) being determined through integration of that peak and normalization for the sample mass.

Films of all POSS TPUs were cast from THF solutions (10% w/v) using the following protocol. Dried polymer (3 g) was dissolved in THF (15 mL), then poured into a PTFE casting dish with a diameter

of 10.5 cm, covered with a glass dish, and left in a chemical hood overnight to evaporate. The film (still in the dish) was then put under vacuum at 50−60 °C for at least 24 h. This process yielded clear, flexible films with a thickness of 0.3 mm, as determined by a digital caliper.

Linear viscoelastic thermomechanical properties of the materials were determined using dynamic mechanical analysis (DMA). A TA Instruments Q800 apparatus was employed in tensile mode with a preload force of 10 mN, amplitude of 15 μm (tensile strain <0.2%), static stress/dynamic stress amplitude ratio ("force tracking") of 108%, and an oscillation frequency of 1 Hz. Samples were cut from the cast films (described above) to feature dimensions of 7 (length) × 1.5 (width) × 0.3 mm (thickness). After loading each film specimen at room temperature under tensile stress, they were cooled to $T = -10$ °C, thermally equilibrated, and finally ramped to 120 °C at a rate of 3 °C/min. For one way shape memory (1W-SM) runs, similar sample dimensions were used, but with a preload force of only 1 mN. The sample was then heated to a deformation temperature of 80 °C, and a force applied ($F = 0.3$ N) at a rate of 0.05 N/min. After being held at the final force for one minute, the sample was cooled down to 10 °C at 3 °C/min and held there for five minutes. The applied force was subsequently unloaded to the initial force of 1 mN at 0.05 N/min and the sample recovered by heating to 80 °C. Multiple cycles were performed on the same film sample and followed the basic procedure of load at 80 °C, cool to 10 °C, unload, and recover to 80 °C.

The same cast films were characterized using wide-angle X-ray diffraction (WAXD). A Rigaku wide-angle X-ray diffractometer (MSC D/Max Ultima) was utilized in reflective mode, enabling quantification of microstructural dimensions of a POSS crystalline phase and an amorphous phase in the TPUs. The instrument was operated at 30 kV and 30 mA using a Cu Kα source ($\lambda = 1.54$ Å). Samples were run at ambient temperature from 5 − 30 °2θ at a scan speed of 0.4 °2θ/min.

In vitro degradation for one of the POSS TPUs was performed by immersing a cut sample (30−40 mg) with typical dimensions of 15 (length) × 5 (width) × 0.3 mm (thickness) in 20 mL PBS buffer containing 0.05% Tween-20. The sample in buffer was held at 37 °C while being constantly agitated at 75 rpm. The buffer for each sample was decanted and replaced with fresh buffer every seven days. At predetermined time points, two samples were retrieved from the buffer, rinsed three times with deionized water, patted dry, and weighed. The samples were then dried for at least 5 days at room temperature under vacuum before being weighed again. The water uptake and mass percent remaining were calculated using the following equations:

$$\text{water uptake } \% = \left(\frac{m_w - m_d}{m_d}\right) \times 100\% \quad (1)$$

$$\text{mass } \% \text{ remaining} = \left(\frac{m_d}{m_{orig}}\right) \times 100\% \quad (2)$$

where m_w is the mass of the wet sample, m_d is the sample after drying under vacuum, and m_{orig} is the mass of the original, nondegraded sample. Dry samples were also used to obtain the molecular weight by GPC. Average values for the two samples are reported herein, with the error bars indicating the actual values (max and min) recorded.

Polyol Synthesis. Polyol (α,ω-polymeric diol) syntheses proceeded by ring-opening polymerization of lactide monomers in the presence of a prescribed concentration of initiating diol and small amount of organometallic catalyst. For the present study, the targeted number-average molecular weight, $\bar{M}_n$, was held fixed at 12 kg/mol, while the initiating PEG molecular weight was varied, dramatically impacting the physical properties of the polyol and resulting TPU.

As a representative example, we describe the detailed procedure to prepare a 12 kg/mol polyol initiated by 1 kg/mol PEG, as polyol given the name **P(1k)LA**. To achieve $\bar{M}_n = 12000$ g/mol, the two poly(D,L-lactide) branches are controlled to have a total molecular weight of 2 × $\bar{M}^{LA}{}_n = 11000$ g/mol. Given that the molar mass of the D,L-lactide monomer is 144 g/mol, 76.4 equivalents of D,L-lactide per PEG initiator are required. In the present example, initiation of 20 g (0.139 mol) of D,L-lactide using **P(1k)** to a total polyol molecular weight of 12 kg/mol, dictated 1.82 g (1.82 mmol) of PEG, yielding 21.82 g of polyol. First, all reactants were dried overnight under vacuum at 50 °C to remove any residual solvent or moisture. Then, 20 g of D,L-lactide monomer was added to a 100 mL Airfree round-bottom flask along with 1.82 g of PEG initiator, following which, nitrogen gas was purged extensively to remove moisture and oxygen. Next, three drops of tin 2-ethylhexanoate were added and the temperature increased to 140 °C over the course of 20 min, during which time the **P(1k)** melted first (~60 °C) followed by the **LA** at higher temperatures (~130 °C). An increase in viscosity was observed after only 1 h at the reaction temperature and progressively increased to a point where magnet stirring with a stir bar was hindered after 10 h. After 12 h of reaction (2 h past gelation), the polymerizing liquid was cooled to room temperature, during which time solidification (vitrification) occurred, and then 55 mL of THF was added and stirring of the solution commenced. Once the polyol dissolved, the pale brown polymer solution was precipitated into an excess of hexanes (~500 mL), leading to a white, stringy product whose consistency ranged from rubbery to sticky, depending on the weight percent of PEG. A total of 20.72 g of polyol product was collected (yield = 95%) and dried under vacuum at 60 °C. Each **P(x)LA** synthesis gave reaction yields of 85% and higher, only varying in the physical properties of the final material; high molecular weight PEG initiator produced a tacky substance that was easily pulled apart, whereas low molecular weight PEG led to a more robust polyol. The nominal molecular weight of the entire polyol ($M_{n,polyol}$) was determined by ^{1}H NMR using the formula

$$M_{n,polyol} = M_{n,PEG} + (DP_{LA} \times 72) \quad (3a)$$

where $M_{n,PEG}$ is the nominal molecular weight of the initiator and DP_{LA} is the degree of polymerization of the lactic acid repeat unit having molecular weight of 72 g/mol (noting that each lactide monomer gives two such repeat units). The DP_{LA} is determined directly from the integration of the resonance from the proton attached to the lactide chiral center (5.1 ppm, 1H) after referencing the PEG peak integration (3.6 ppm) to be the total number of protons present in the initiator, as defined in eq 3b.

$$A_{PEG} = \frac{M_{n,PEG}}{44} \times 4 \quad (3b)$$

where 44 refers to the repeat unit of PEG (44 g/mol) and 4 refers to the number of protons per repeat unit of PEG. GPC characterization was run on the dried products, confirming the desired polyol structure had a unimodal distribution of molecular weights.

TPU Synthesis. TPU syntheses were conducted by reacting the polyol **P(1k)LA** (synthesis above) with varying molar ratios of POSS diol using a lysine-derived diisocyanate (**LDI**) and typical urethane chemistry. The feed POSS/polyol ratios used were 0:1, 1:1, 2:1, and 3:1, although actual yield ratios (as determined by ^{1}H NMR, shown below) were found to be lower than expected when increasing amounts of POSS were used. Still, a dramatic change in material properties could be seen among the final TPUs with even slight variations of the POSS/polyol ratio. An example of the TPU synthesis using **P(1k)LA** and a POSS/polyol ratio of 1:1 is as follows (sample name **P(1k)LA-P1**). A total of 3 g (0.249 mmol, molecular weight as determined by ^{1}H NMR) of polyol and 0.26 g (0.249 mmol) POSS diol were added to a three-necked 50 mL round-bottom flask, following which dry toluene was added to yield a 40% (w/v) solution that was purged with nitrogen exhaustively to remove moisture and oxygen. After a clear solution was obtained at 50 °C (~1 h), 0.096 mL (0.523 mmol) of purified LDI liquid was added dropwise over the span of 2 min for a total addition in slight molar excess isocyanate/alcohol of 1.05:1.00. Following complete addition of the LDI, three drops (ca. 0.01 mL) of dibutyltin dilaurate were added with stirring. The reaction temperature was then increased to 90 °C and stirring was continued for 6 h. A significant increase in viscosity was observed during polymerization, therefore, 5 mL of additional toluene was added prior to precipitation of the final

Table 1. Material Properties of the Lactide-Based Polyols Initiated by Different Molecular Weight PEG

samples	M_n[a] (g/mol)	M_n[b] (g/mol)	PDI[b]	PEG wt % (x[a]) (y[b])	T_g (°C)	$T_{m,PEG}$ (°C) [ΔH (J/g)]
P(0.6k)LA	13200	11800	1.28	4.6 (5.1)	32.8	n/a
P(1k)LA	11800	9300	1.25	8.5 (10.8)	29.1	n/a
P(2k)LA	11,300	9000	1.18	17.6 (22.2)	15.1	n/a
P(4k)LA	10400	10400	1.12	38.5 (38.5)	−16.8	34.3 [1.096]

[a] Based on ^{1}H NMR. [b] Based on light scattering from GPC.

Table 2. Summary of Material Properties for POSS TPUs Made from P(1k)LA Polyol with Increasing Amounts of POSS in the Hard Block

samples	M_w[a] (g/mol)	PDI	POSS/polyol ratio[b]	wt % hard block	T_g (°C)	$T_{m,POSS}$ (°C) [ΔH (J/g)]
P(1k)LA-P0	50200	1.35	0	0	27.8	
P(1k)LA-P1	106500	1.35	0.98	10.7	34.5	112.8 [0.35]
P(1k)LA-P2	87200	1.36	1.67	15.2	34.4	118.0 [0.98]
P(1k)LA-P3	101000	1.39	2.63	20.8	35.5	116.1 [1.5]

[a] Based on light scattering from GPC. [b] Based on ^{1}H NMR.

Scheme 1. Synthetic Route for the Preparation of Polyesters Made from D,L-Lactide and Initiated by Poly(ethylene glycol) of Varying Molecular Weights

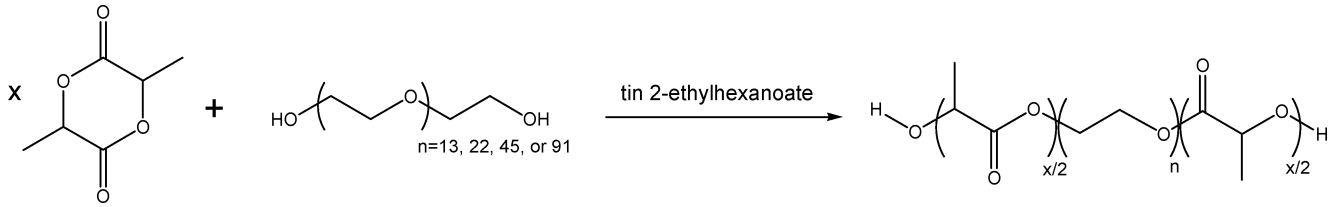

product into a 10-fold excess of hexanes. The precipitate was well-defined, clear strings of polymer that clumped together into a ball during stirring. Unlike the polyol precipitate, which smeared out under shear forces from the stir bar, the TPU product maintained its as-precipitated shape, unless heated above POSS melting (~120 °C), as will be described below. The final product was collected by filtration and dried under vacuum at 60 °C yielding 3.27 g of **P(1k)LA-P3** or 97% polymerization yield. Other TPU polymerizations proceeded in the same manner, with yields spanning 81−97%. Lower yields were obtained from the higher POSS/polyol feed ratios due to actual POSS inclusion becoming more difficult as the hard block weight percent was increased, as will be discussed below. GPC was used to determine molecular weight, while ^{1}H NMR ratios (see below) were used to measure the final POSS/polyol ratio.

TPU Composition Measurements. A solution ^{1}H NMR method was employed to measure the level of POSS incorporation in the TPUs, specifically the POSS/polyol ratio. For this purpose, we considered the integration of resonances in the ^{1}H spectra: A_{POSS} for the POSS moiety (0.9 ppm; 6 per POSS), A_{LA} for the D,L-lactide repeating unit in the polyol (5.1 ppm; 1 per repeat unit). The ratio of these integrations yields the relative levels of POSS and lactide incorporated in the TPU through the relation

$$\frac{A_{POSS}}{A_{LA}} = \frac{H_{POSS}N_{POSS}}{H_{LA}N_{LA}} = \frac{42}{1}\frac{N_{POSS}}{(N_{polyol}DP_{LA})} \quad (4)$$

where H_{POSS} and H_{LA} are the number of protons per proton-bearing group assessed (42 methyl protons per POSS and 1 methine proton per lactide), and DP_{LA} is the number of lactide repeating units per polyol (as discussed in the polyol section above). Defining the POSS/polyol ratio as $x = N_{POSS}/N_{polyol}$, we arrive at the following relationship relating the desired quantity x to our directly measured quantities

$$\frac{A_{POSS}}{A_{LA}} = x\frac{42}{1}\frac{72}{(M_{n,polyol} - 1000)} \quad (5)$$

A sample ^{1}H NMR spectrum, along with significant peak assignments can be found in the Supporting Information (Figure S1). The POSS/polyol ratio, x, was measured and recorded for each of our POSS TPUs. This ratio also gives an *average* value for the degree of polymerization of the hard block, meaning number of sequential POSS units attached between two polyol blocks.

It will be helpful to consider the hard block wt % in the TPUs, W_H. This is related to x and the molar masses involved as

$$W_H = \frac{xM_{POSS} + (x+1)M_{LDI}}{M_{n,polyol} + xM_{POSS} + (x+1)M_{LDI}} \quad (6)$$

where M_{POSS} and M_{LDI} are 1052 and 212.2 g/mol, respectively. W_H values measured in this manner are tabulated (Table 2) and discussed in the context of the thermomechanical data for the TPU series.

Results and Discussion

Polyol Characterization. Soft block polyols for subsequent incorporation into a series of polyurethanes were synthesized by ring opening polymerization of D,L-lactide monomer initiated by poly(ethylene glycol)s of varying length, as shown in Scheme 1. Alternate vacuum and nitrogen purges were used to suppress any side reactions from air/moisture contamination and ensure the target molecular weight was obtained. Success for each reaction was measured by how closely the material came to the desired M_n value of 12 kg/mol, as determined by ^{1}H NMR characterization (method described above) and shown in Table 1. Although the M_n was also determined by light scattering from GPC, values obtained were always ~2 kg/mol lower than those from NMR (except for **P(4k)LA**). To stay consistent with NMR calculation assumptions used for the POSS/polyol ratio of the polyurethanes, only NMR-determined M_n values are considered. All values are relatively close to the target M_n, ranging from 10.4 kg/mol to 13.2 kg/mol, and fluctuations can be explained by the use of the PEG initiator M_n stated from the manufacturer being a nominal/rounded value from a precise measurement, which would alter stoichiometry. Regardless, polydispersity, as determined by GPC, was low for each polyol (<1.3) and gave expected values for this well-documented type of synthesis. The

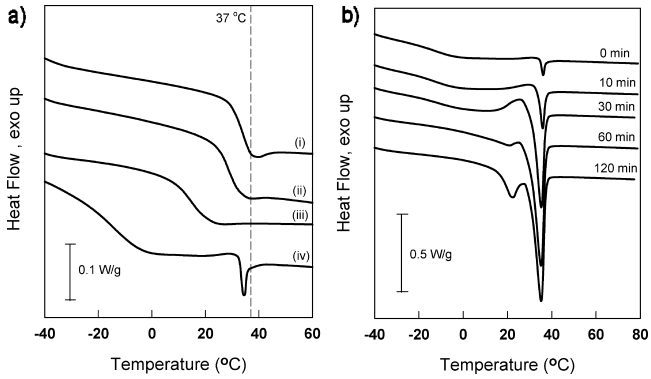

Figure 1. DSC second heating traces for (a) **P(x)LA** polyols initiated by PEG with molecular weights of (i) 600 g/mol, (ii) 1 kg/mol, (iii) 2 kg/mol, (iv) 4 kg/mol; and (b) **P(4k)LA** with various annealing times at 10 °C showing the crystallization of the PEG block.

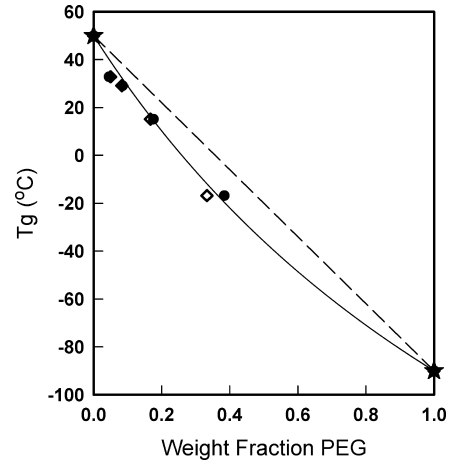

Figure 2. Change in T_g for **P(x)LA** polyols with different molecular weight PEG initiator as calculated from an ideal 12 kDa composition (◇) and using molecular weight determined by NMR (●). PEG 0% (all lactide)[63] and PEG 100% (M_w = 10 kg/mol)[64] T_g values are taken from the indicated references. The dashed line connects the two extremes and represents the Fox equation. The curved solid line is a fit to the Gordon−Taylor equation.

NMR-determined molecular weights and nominal PEG initiator molecular weights were also used to determine the weight percentage of PEG in each material. Values increased from ~5% to as much as 40%, drastically affecting the observed glass transition temperature (T_g) of the polyol, as will be discussed below.

As expected, increasing the content of more flexible PEG in the lactide soft block served to decrease the glass transition temperature,[61−63] as shown in Figure 1a (values in Table 1). The once sharp transition of **P(0.6k)LA** becomes substantially broadened, with the heat flow step spanning an increasing temperature range with increasing PEG content. Despite the triblock architecture, complete miscibility of the amorphous D,L-lactide and short PEG blocks is evident by the single transition, seen up through the **P(2k)LA** sample. **P(4k)LA**, containing almost 40 wt % PEG, displays a second transition at $T \approx 34$ °C, featuring an endothermic peak superimposed on a small step-down in heat flow (step-up in heat capacity). Upon first consideration, the dip of the baseline suggests the formation of a second T_g coupled with an aging peak due to the transition existing close to, but above, room temperature. This would further indicate that the poly(D,L-lactide) and PEG blocks are microphase separated, with the PEG block exhibiting the lower (subzero) T_g and poly(D,L-lactide) having an apparent T_g closer to that of pure poly(D,L-lactide) (~50 °C).[63]

To better understand the nature of the higher temperature transition(s), **P(4k)LA** samples were subjected to DSC cooling runs of varying rates: 20, 10, 5, 3, and 1 °C/min. For a conventional glass transition, slower cooling rates lead to slightly lower glass transition measurements, owing to the kinetic nature of the transition itself. In fact, no change was observed in any of the traces, except for 1 °C/min showing a larger "aging" peak, relative to that of Figure 1a upon subsequent heating (data not shown). Next, using a constant cooling and heating rate of 10 °C/min, cooling was interrupted for annealing at $T = 10$ °C for varying amounts of time and then continued to $T = -50$ °C, following which a heating run was executed to evaluate the resulting phase behavior. The annealing condition was chosen based on its position halfway between the lower T_g centered at $T = -10$ °C and the higher complex transition beginning at 30 °C. Although no exotherm had been previously witnessed during cooling runs of the **P(4k)LA** polyol, we reasoned that annealing at 10 °C would allow for crystallization that was potentially kinetically hindered during previous cooling runs. As seen in Figure 1b, the peak grows to consist of two separate endothermic transitions: one with a peak centered at 22.5 °C and the other centered at 35.2 °C. Inspecting the sequence of thermograms in Figure 1b, it is evident that the lower endothermic transition is slower to grow, eventually eclipsing a residual heating exotherm associated with growth of the larger endotherm. Importantly, the DSC thermogram of the 4 kg/mol PEG itself (not **P(4k)LA**) revealed the exact same "double melt" behavior but at a higher temperature close to 60 °C (Supporting Information).

The observed melting for the **P(4k)LA** materials indicates that a critical weight percent of PEG is required for segregation of poly(D,L-lactide) and PEG blocks and subsequent crystallization of PEG. A similar finding has been reported previously for ABA triblocks with PEG content approaching 40%.[61] The T_g value obtained after each of the annealing experiments also increased with annealing time, from −17 to −10 °C before becoming indistinguishable with the melting endotherm, indicating enhanced segregation associated with PEG block crystallization.

For our polyol series, direct manipulation of T_g was afforded by varying the weight fraction of PEG in the material via the molecular weight of the PEG initiator. As shown in Figure 2, the polyol T_g drops monotonically and dramatically with increasing weight fraction of PEG, in this case, dictated by the PEG initiator molecular weight. Further, we see from Figure 2 that the experimental data were fit well by the Gordon−Taylor (GT) equation, eq 7, applied here for block copolymers instead of the conventional miscible blends.

$$T_g^{cop} = \frac{w_1 T_{g,1} + k w_2 T_{g,2}}{w_1 + k w_2} \tag{7}$$

Indeed, data for the **P(4k)LA** sample was employed in the fitting, using the pronounced T_g evident in Figure 1a (before annealing), despite some evidence for microphase separation in that system. Further, T_g values of 50 °C[63] and −90 °C[64] were taken for pure poly(D,L-lactide) and PEO, respectively. These restrictions given and using T_g values in Kelvins, eq 7 was curve-fit to the data of Figure 2 allowing determination of the GT k value of 0.63 ± 0.05 (best fit estimate) with an R^2 value of 0.995. We note that the required PEG weight fraction values, the abscissa in Figure 2, are determined using the nominal PEG molecular weight from the supplier and the total polyol molecular weight, as determined by ^{1}H NMR, or from an "ideal"

Scheme 2. Preparation of POSS-TPUs Made by Reacting the Polyol P(1k)LA with a Lysine-Derived Diisocyanate and POSS Diol

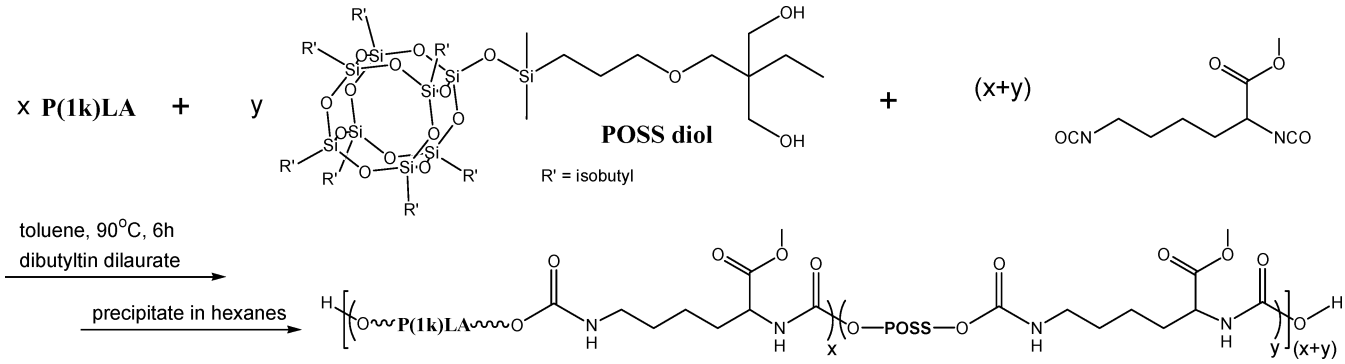

molecular weight of 12 kg/mol. The slight differences translate to the uncertainty in the fitting that we indicate above.

It has previously been asserted that the Gordon−Taylor k value can be used to estimate the interaction between components of a blend,[65,66] or in this case copolymer blocks, with $k > 1$ indicating favorable mixing. For the polyol samples, the calculated k value is closer to 1 than 0, indicating some favorable interactions are taking place, most likely in the form of hydrogen bonding, though proving this will require spectroscopic investigation beyond the scope of our present study. Knowing the GT parameters allows prediction of the PEG weight fraction (and thus PEG molecular weight in our architecture) required for a target transition temperature per the intended application. For example, our results and GT fitting predict a required PEG content of 7% (840 g/mol) or 14.7% (1764 g/mol) for a desired T_g of 35 or 20 °C, respectively. As will be discussed later, polyol composition is the main factor influencing the primary softening transition in the final polyurethane. As such, control over the soft block synthesis is crucial in obtaining a final product with specifically tuned properties. Given our stated objective to achieve medically relevant biodegradable shape memory polymers, we hereafter restrict the TPU composition to those incorporating the **P(1k)LA** soft block. This polyol is ideal for biomedical applications due to its moderate T_g and increased hydrophilicity from the PEG component as compared to a purely lactide polymer.

TPU Characterization. **P(1k)LA** was used to prepare thermoplastic polyurethanes containing POSS by an alcohol-isocyanate polyaddition with lysine-diisocyanate (LDI) and various molar equivalents of POSS diol, serving as chain extender (Scheme 2). In all cases, a slight molar excess of isocyanate compared to alcohol groups was used. Molecular weight (M_w) values (Table 2) for the POSS-containing TPUs, **P(1k)LA-P1**, **-P2**, and **-P3**, were between 85 and 110 kg/mol with polydispersities below 1.4. The non-POSS analogue, **P(1k)LA-P0**, made by reacting 1:1 molar ratios of polyol and diisocyanate, also gave a low PDI value of 1.35, but was lower in molecular weight. Because this reaction contains none of the short chain extender (POSS diol), it is likely that the decreased mobility of the larger polyol chains, compared to that of the POSS monomer, resulted in fewer reactive end groups coming in proximity to each other on the time scale of the reaction (6 h). For reactions in which POSS was included, the POSS/polyol feed ratio, as indicated by the final number in each polymer's naming scheme, was not always what was observed in the resulting product. As described above, ^{1}H NMR was used to determine the final ratio and was found to be closer to the feed ratio for low POSS inclusion, such as was seen for **P(1k)LA-P1**. For **P(1k)LA-P2** and **P(1k)LA-P3**, only an average of 85% of the POSS in the reaction flask was included in the final product, indicating that POSS inclusion becomes more difficult as the amount of POSS increases. The lowered inclusion is most likely a factor of the bulky POSS molecules experiencing steric hindrance when trying to pack together using the short LDI spacer. This phenomena was also evidenced in the % yield from the TPUs with higher POSS/polyol feed ratios, which was typically 10% less than the low and non-POSS TPUs (avg 83% versus avg 94%). When the NMR-determined POSS/polyol ratios were used, the weight percent of the POSS hard block was calculated using eq 6. Values ranged from zero (**P(1k)LA-P0**) to ∼21% (**P(1k)LA-P3**) and will be discussed below in terms of physical properties of the materials.

TPU Physical Properties. The TPUs whose synthesis and molecular characterization details are described above were further processed by solution-casting into films from THF for analysis of their physical properties, beginning with thermal analysis. The glass transition temperature (T_g) and melting temperature (T_m) values were each determined by DSC, using the second heating runs so as to first erase all previous thermal history. This was accomplished by heating samples to 160 °C and holding for five minutes before cooling to −50 °C and commencing with the second heating run. The results are shown in Figure 3 and tabulated in Table 2. For the non-POSS TPU, **P(1k)LA-P0**, the glass transition temperature was found to be very similar (within 1 °C) to that of the polyol it was synthesized from and no melting was observed. Importantly, all POSS-containing TPU samples showed T_gs around 35 °C, which is only 6 °C higher than that of the original polyol T_g of 29 °C. The slight increase may be due to some soft block confinement when the hard block is present, but the total hard block weight percent is not a controlling factor. Specifically, increasing the

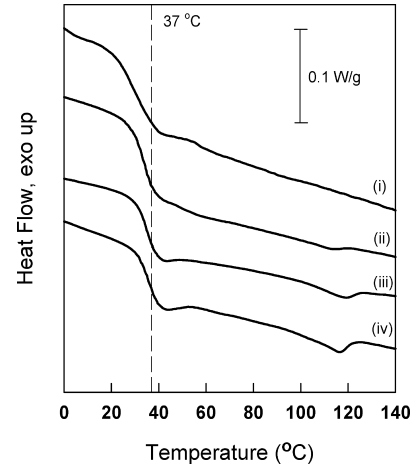

Figure 3. DSC second heating traces for (i) **P(1k)LA-P0**, (ii) **P(1k)LA-P1**, (iii) **P(1k)LA-P2**, and (iv) **P(1k)LA-P3**.

weight percent of the hard block from 10 to 20% (hard block to soft block ratio from 0.98 to 2.63) only increases T_g by about 1 °C, showing little to no influence from the amount of POSS in the hard block. Also, the step in heat capacity at the transition (ΔC_p) scales directly with the weight percentage of polyol, decreasing from 0.591 J/(g°C) for the 100% amorphous, non-POSS TPU to 0.562, 0.498, and 0.483 J/(g°C) as the polyol content decreased to 89.3, 84.8, and 79.2%, respectively. The near constancy in T_g from polyol to TPU, along with ΔC_p scaling with W_H, indicates that the POSS-containing TPUs exist in a microphase-separated state and that the soft block undergoes a glass transition. This type of behavior corresponds well with that of other microphase-separated multiblock copolymers.[12,67]

The POSS-rich hard block is semicrystalline, with a heat-of-fusion that increases with POSS/polyol ratio, x, and hard block weight fraction, W_H. This is clearly evidenced in Figure 3 where a small and broad endothermic transition appears for **P(1k)LA-P1** over the range 100−120 °C, but becomes larger and more defined as W_H increases from 10 to 20%. For the same range of W_H, the melting temperature also increases from 113 to 118 °C, approaching the pure POSS T_m of 130 °C (see Supporting Information for DSC of the POSS diol). Further increase in W_H, however, did not further increase T_m. The melting endotherm is fairly broad and can be correlated with the synthetic technique used to make these polymers. Due to the "one-pot, one step" method employed, it was expected that the TPUs would feature heterogeneity in the hard block DP. Within the same sample, it is thought that the crystalline hard block domains can be made up of single POSS units flanked by polyol self-assembling into a two-dimensional "double raft" structure, as was seen for polyethylene-POSS copolymers[31] or multiple POSS units linked together by LDI assembling into thicker raft structures. The variation in POSS crystal type would lead to a wide range of melting temperatures which all combine to create one broad endotherm. Regardless, POSS crystallizing in a hard block is significant, since past research on POSS random copolymers revealed POSS aggregation, but not POSS crystallization, while the POSS-PEO telechelic architecture[29] and the methacryl-POSS-butacrylate-methacrylPOSS triblock architectures[28] both allowed crystallization. Thus, architecturally sequestering POSS along the backbone appears requisite for crystallization.

To further clarify the microstructure of our POSS TPUs after processing, wide-angle X-ray diffraction studies were conducted on solution-cast films with the diffractograms compared to the pure POSS diol. The results are shown in Figure 4. For the POSS diol monomer, we observe strong characteristic diffraction peaks at scattering angles of $2\theta = 7.9$, 10.6, and 18.6° corresponding to d-spacing values of 11.18, 8.34, and 4.76 Å, respectively. These values are similar to those found by Waddon[68] with slight variations due to the difference in vertex R groups (isobutyl versus cyclopentyl) and also agree with their conclusion of a hexagonal crystal lattice. The POSS crystal structure in an amorphous matrix has also been discussed in terms of a rhombohedral[55] morphology, but the in-depth X-ray analysis required for this determination is beyond the scope of this paper. As POSS content is increased in the TPUs, the X-ray diffraction peak corresponding to the POSS monomer reflection at 7.9° is the first to emerge from the amorphous halo witnessed for **P(1k)LA-P0**. Uniformly, this peak in the TPUs is shifted slightly to a larger diffraction angle (8.05°, d-spacing = 10.97 Å) when compared to the same peak for the 3D crystal (7.9°, d-spacing = 11.18 Å). The closer packing of POSS units in the TPU as compared to that of the pure POSS diol may be a result

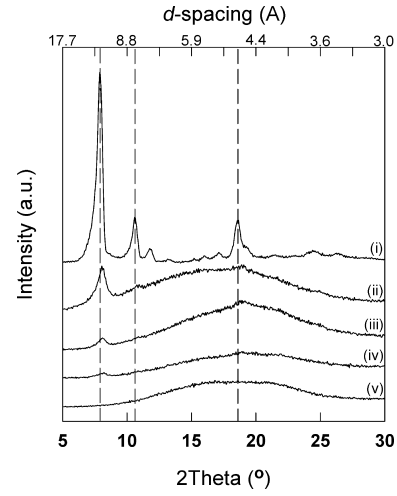

Figure 4. WAXD of (i) POSS diol monomer, (ii) **P(1k)LA-P3**, (iii) **P(1k)LA-P2**, (iv) **P(1k)LA-P1**, and (v) **P(1k)LA-P0**.

of the surrounding amorphous matrix imposing constraints on the crystal size. In the POSS monomer case, but with a larger vertex group (cyclohexyl), this peak corresponded to the *101* lattice spacing of a rhombohedral unit cell with inclination angle $\alpha \approx 95.5°$.[55] As the POSS content increases, the two other prominent POSS diffraction peaks at 10.6° (8.34 Å) and 18.6° (4.76 Å) are revealed. These diffractions are consistent with the general trend seen in DSC where increasing the POSS content led to increased crystallinity of the entire material. On the other hand, WAXD observations proved insensitive to the difference between crystals formed by single-POSS unit hard blocks and multiple-POSS unit hard blocks which contributed to the broad melting manifested in DSC.

Recalling our interest in development of biodegradable shape memory polymers, of paramount importance is the control of thermo-mechanical properties, particularly TPU elastic moduli and transition temperatures. As such the TPUs based on the **P(1k)LA** polyol were compared with one another using dynamic mechanical analysis (DMA) in tensile mode. After mounting each sample in the DMA tensile grips at ambient temperature, they were then cooled to −10 °C and ramped up to 120 °C (or until the sample yielded) at 3 °C/min while being subjected to a small oscillatory strain at a frequency of 1 Hz while measurements of tensile storage modulus and loss tangent were made. The results are shown in Figure 5. We observe that all POSS-containing TPUs feature a storage tensile modulus greater than 2 GPa at low temperature, but that this modulus dramatically drops to a value of about 10 MPa upon heating above T_g. This rubbery plateau of modulus is quite broad in temperature for all POSS TPUs, effectively bridging the temperature range spanning the soft block T_g and hard block T_m, while the **P(1k)LA-P0** sample softened continuously upon heating above T_g. Considered in light of the DSC and WAXD data, it is apparent that the POSS hard block crystallization provides the physical cross-linking required for elastic mechanical behavior.

Considering further our interest in controlled shape recovery in the narrow range spanning 37−50 °C (physiological to tissue-burning), it is significant that all of the POSS TPUs studied begin and end their softening transition over this range of temperatures. Given the close correlation between the primary softening transition breadth and the breadth for shape recovery in the shape memory cycle,[14] we fully anticipate shape recovery for these samples in a temperature range ideal for implantable

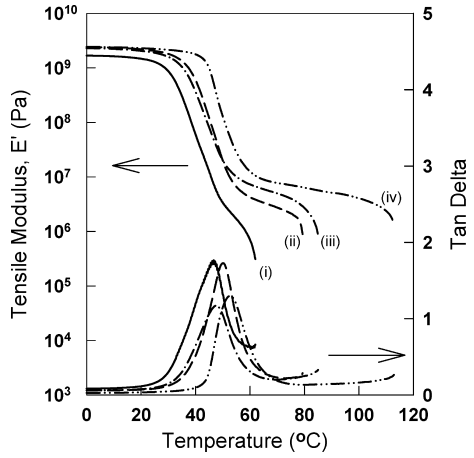

Figure 5. Storage tensile modulus measurements for TPUs with different POSS loadings: (i) **P(1k)LA-P0**, (ii) **P(1k)LA-P1**, (iii) **P(1k)LA-P2**, and (iv) **P(1k)LA-P3**.

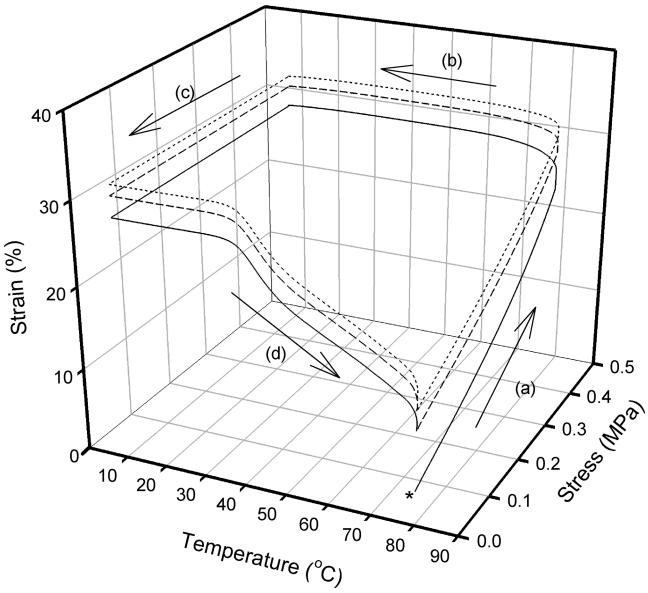

Figure 6. One-way shape memory cycles for **P(1k)LA-P3**. Three cycles are shown: (—) first cycle, (– –) second cycle, and (- - -) third cycle. The asterisk marks the beginning of the cycle and the arrows denote the various stages, specifically (a) deformation, (b) cooling/fixing, (c) unloading, and (d) recovery.

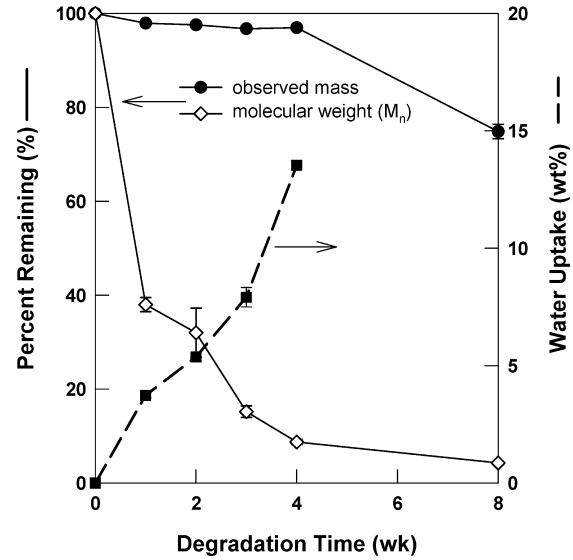

Figure 7. Degradation profile for **P(1k)LA-P3**, including percent observed mass remaining (●), percent number-average molecular weight (M_n) remaining (◊), and weight percent water uptake (■).

medical devices and surgical tools. The extent of the rubber plateau for the TPU samples was limited on the high temperature side by yielding of samples under the action of the required static stress of approximately 6.5 MPa. One exception was **P(1k)LA-P3**, which was a particularly robust sample that maintained its original rectangular geometry until the highest temperature tested (120 °C). Qualitatively, the non-POSS control sample, **P(1k)LA-P0**, was quite tough at room temperature, but quantitatively displayed a lower modulus of 1.5 GPa below T_g and an absence of any rubbery plateau. The absence of a rubbery plateau prevented the non-POSS TPU from exhibiting any quantifiable shape memory properties due to the lack of a recovery driving force, such as is afforded with physical or chemical cross-links.

The robust **P(1k)LA-P3** material was further investigated for its one-way shape memory properties. Figure 6 shows three cycles of the shape memory program. The sample was heated to 80 °C ($T > T_g$) and deformed (a) by ramping to a load of 0.3 N. The sample was then cooled under this load (b) to 10 °C, during which period the soft block chains vitrified and fixed the sample into a temporary, elongated shape. Next, the sample was unloaded (c) and subsequently heated/recovered (d) to 80 °C. The first cycle shows ~5% creep occurring between the elongation and fixing step over a period of 5 min. Excellent shape fixing of >99% is observed for the first and each subsequent cycle meaning that none of the induced strain is lost once the applied load is removed. Recovery is not complete for the first cycle and achieves about 71% of the original strain. Both creep and recovery improve on each subsequent cycle: creep decreases to 3% and 2.5% and recovery increases to 89% and 93% for cycle two and three, respectively. Because the shape memory cycle was run on the as-cast film, it is expected that optimally annealing the film and allowing the POSS domains to grow would reduce the number of initial "training" cycles required before ideal properties are obtained, that is, no creep and 100% recovery. It should be noted that the temperature used here for recovery is higher than the physiologically-friendly conditions discussed earlier, although it is believed that hydration of the sample in aqueous conditions will serve to lower the glass transition temperature further and, therefore, lower the recovery temperature required. Also, the sample could be held at a desired temperature ($T = T_g + 5$, 10, 15 °C, etc) and then allowed to recovery over a certain period of time. Investigation into both of these approaches to understand the shape recovery properties of the POSS TPUs is currently underway.

Finally, we examined the in vitro degradation profile for **P(1k)LA-P3** in terms of mass loss, molecular weight change, and water uptake. Due to the polylactide-based soft block in the TPUs, it was expected that the sample would undergo bulk degradation through hydrolysis of the ester bonds, although the degradation could be somewhat altered due to the presence of hydrophobic, nondegrading POSS. Rectangular cut pieces of the cast film were incubated in PBS buffer at 37 °C over a 2 month period and samples were collected at weeks 1–4 and week 8. As shown in Figure 7, less than 4% of the original mass was found to elute from the sample after a month in the buffer, most likely from chain ends on the surface of the sample undergoing hydrolysis. Although only a small mass loss was observed, the molecular weight of the samples dropped dramatically after only one week to ~40% of the original value. The

molecular weight continued to decrease, albeit at a slower rate, until only 10% of the original number-average molecular weight, ~8 kg/mol, remained after four weeks. This molecular weight was revealed to be close to the critical value for large mass loss and gave rise to a 20% mass loss between weeks 4 and 8. Water uptake was moderate for **P(1k)LA-P3**, indicating low swelling, and remained below 15 wt % even with large chain scission. While the sample remained intact throughout the degradation, the week 8 films became delicate and broke upon handling. For this reason, the water uptake was not determined after week 4 so that an accurate mass loss could be obtained (i.e., handling of the sample was minimized so that no pieces were inadvertently lost). Overall, **P(1k)LA-P3** was found to have a favorable degradation profile, with an incubation period of more than one month before bulk mass loss occurred and no observable swelling.

Conclusions

New biodegradable thermoplastic polyurethanes incorporating POSS have been synthesized using a two-step technique. The initial step, synthesis of the lactide-based soft block, allowed for manipulation of the glass transition temperature through controlled PEG inclusion. Synthesis of the subsequent polyurethane using POSS as the hard block allowed for mechanical stability, due to physical cross-links of the crystalline POSS domains, to an extent usually not seen in degradable, nonchemically cross-linked systems. After varying the POSS/polyol ratio from 0:1 to 3:1, it was found that a ratio of 3:1 gave the most robust properties due to the material being semicrystalline, but still flexible during elongation. The non-POSS analogue containing no hard block proved to be mechanically inferior, failing much earlier during tensile tests than the POSS-incorporating samples and having a lower tensile modulus both above and below T_g. The **P(1k)LA-P3** showed moderate shape memory properties that increased during cycling. This sample was also observed to undergo in vitro bulk degradation through chain scission of the soft blocks leading to mass loss of the bulk film after two months. Water uptake of the sample was low (<15 wt %) even when the molecular weight had dropped to only 10% of the original value. In vivo biocompatibility and degradation studies of the **P(1k)LA-P3** sample and analogous POSS TPU materials is currently underway and will be discussed in future publications.

Acknowledgment. The authors gratefully acknowledge Boston Scientific Corporation for supporting this work through a graduate fellowship to P.T.K.

Supporting Information Available. NMR spectrum for a sample polymer, **P(1k)LA-P2**, with characteristic peaks labeled; DSC second heating traces for (i) **PEG(4k)** homopolymer and (ii) **P(4k)LA** annealed at 10 °C on the cool for 120 min: each exhibit double-melting behavior; and (3) DSC first cooling (after melting at 160 °C) and second heating traces for TMP POSS diol. This material is available free of charge via the Internet at http://pubs.acs.org.

References and Notes

(1) Kumar, N.; Ravikumar, M. N. V.; Domb, A. J. *Adv. Drug Delivery Rev.* **2001**, *53* (1), 23–44.
(2) Vert, M. *Biomacromolecules* **2005**, *6* (2), 538–546.
(3) Kricheldorf, H. R. *J. Polym. Sci., Part A: Polym. Chem.* **2004**, *42* (19), 4723–4742.
(4) Wang, S.; Cui, W.; Bei, J. *Anal. Bioanal. Chem.* **2005**, *381* (3), 547–556.
(5) Deng, X. M.; Xiong, C. D.; Cheng, L. M.; Xu, R. P. *J. Polym. Sci., Part C: Polym. Lett.* **1990**, *28* (13), 411–16.
(6) Wang, Z.-Y.; Zhao, Y.-M.; Wang, F. *J. Appl. Polym. Sci.* **2006**, *102* (1), 577–587.
(7) Cho, H.; Chung, D.; Jeongho, A. *Biomaterials* **2004**, *25* (17), 3733–3742.
(8) Kim, M. S.; Hyun, H.; Khang, G.; Lee, H. B. *Macromolecules* **2006**, *39* (9), 3099–3102.
(9) Hyun, H.; Kim, M. S.; Jeong, S. C.; Kim, Y. H.; Lee, S. Y.; Lee, H. B.; Hyun, H.; Khang, G. *Polym. Eng. Sci.* **2006**, *46* (9), 1242–1249.
(10) Wang, W.; Ping, P.; Chen, X.; Jing, X. *J. Appl. Polym. Sci.* **2007**, *104*, 4182–4187.
(11) Sanchez-Adsuar, M.; Papon, E.; Villenave, J. *J. Appl. Polym. Sci.* **2000**, *76* (10), 1602–1607.
(12) Chen, K. S.; Yu, T. L.; Tseng, Y. H. *J. Polym. Sci., Part A: Polym. Chem.* **1999**, *37* (13), 2095–2104.
(13) Asplund, J. O. B.; Bowden, T.; Mathisen, T.; Hilborn, J. *Macromolecules* **2006**, *39* (13), 4380–4385.
(14) Liu, C.; Qin, H.; Mather, P. T. *J. Mater. Chem.* **2007**, *17* (16), 1543–1558.
(15) Lendlein, A.; Kelch, S. *Angew. Chem., Int. Ed.* **2002**, *41* (12), 2034–2057.
(16) Medical Applications of Hybrid Materials. *Hybrid Materials. Synthesis, Characterization, and Applications*., Kickelbick, G., Ed.; Wiley: Weinheim, Germany, 2007; Ch. 8, pp 301−335.
(17) Deng, Q.; Moore, R. B.; Mauritz, K. A. *J. Appl. Polym. Sci.* **1998**, *68* (5), 747–763.
(18) Grady, B. P.; Start, P. R.; Mauritz, K. A. *J. Polym. Sci., Part B: Polym. Phys.* **2000**, *39* (2), 197–200.
(19) Young, S. K.; Jarrett, W. L.; Mauritz, K. A. *Polymer* **2002**, *43* (8), 2311–2320.
(20) Naik, R. R.; Brott, L. L.; Clarson, S. J.; Stone, M. O. *J. Nanosci. Nanotechnol.* **2002**, *2* (1), 95–100.
(21) Rodriguez, F.; Glawe, D. D.; Naik, R. R.; Hallinan, K. P.; Stone, M. O. *Biomacromolecules* **2004**, *5* (2), 261–265.
(22) Fu, G.; Valiyaveettil, S.; Wopenka, B.; Morse, D. E. *Biomacromolecules* **2005**, *6* (3), 1289–1298.
(23) Wustman, B. A.; Weaver, J. C.; Morse, D. E.; Evans, J. S. *Langmuir* **2003**, *19* (22), 9373–9381.
(24) Kannan, R. Y.; Salacinski, H. J.; Butler, P. E.; Seifalian, A. M. *Acc. Chem. Res.* **2005**, *38* (11), 879–884.
(25) Lichtenhan, J. D.; Otonari, Y. A.; Carr, M. J. *Macromolecules* **1995**, *28* (24), 8435–7.
(26) Lichtenhan, J. D.; Vu, N. Q.; Carter, J. A.; Gilman, J. W.; Feher, F. J. *Macromolecules* **1993**, *26* (8), 2141–2.
(27) Schwab, J. J.; Lichtenhan, J. D.; Carr, M. J.; Chaffee, K. P.; Mather, P. T.; Romo-Uribe, A. *Polym. Mater. Sci. Eng.* **1997**, *77*, 549–550.
(28) Pyun, J.; Matyjaszewski, K.; Wu, J.; Kim, G.-M.; Chun, S. B.; Mather, P. T. *Polymer* **2003**, *44* (9), 2739–2750.
(29) Kim, B.-S.; Mather, P. T. *Macromolecules* **2006**, *39* (26), 9253–9260.
(30) Constable, G. S.; Lesser, A. J.; Coughlin, E. B. *Macromolecules* **2004**, *37* (4), 1276–1282.
(31) Waddon, A. J.; Zheng, L.; Farris, R. J.; Coughlin, E. B. *Nano Lett.* **2002**, *2* (10), 1149–1155.
(32) Zheng, L.; Kasi, R. M.; Farris, R. J.; Coughlin, E. B. *Polym. Mater. Sci. Eng.* **2001**, *84*, 114–115.
(33) Li, G. Z.; Cho, H.; Wang, L.; Toghiani, H.; Pittman, C. U., Jr. *J. Polym. Sci., Part A: Polym. Chem.* **2004**, *43* (2), 355–372.
(34) Patel, R. R.; Mohanraj, R.; Pittman, C. U., Jr *J. Polym. Sci., Part B: Polym. Phys.* **2005**, *44* (1), 234–248.
(35) Zhang, Y.; Lee, S. H.; Yoonessi, M.; Toghiani, H.; Pittman, C. U., Jr *J. Inorg. Organomet. Polym.* **2007**, *17* (1), 159–171.
(36) Asuncion, M. Z.; Laine, R. M. *Macromolecules* **2007**, *40* (3), 555–562.
(37) Choi, J.; Kim, S. G.; Laine, R. M. *Macromolecules* **2004**, *37* (1), 99–109.
(38) Suresh, S.; Zhou, W.; Spraul, B.; Laine, R. M.; Ballato, J.; Smith, D. W., Jr *J. Nanosci. Nanotechnol.* **2004**, *4* (3), 250–253.
(39) Haddad, T. S.; Lichtenhan, J. D. *Macromolecules* **1996**, *29* (22), 7302–7304.
(40) Li, G.; Pittman, C. U., Jr *Macromol. Containing Met. Met.-Like Elem.* **2005**, *4*, 79–131 (Group IVA Polymers).
(41) Qin, H.; Mather, P. T. *PMSE Preprints* **2006**, *94*, 127–128.
(42) Schwab, J. J.; Lichtenhan, J. D. *Appl. Organomet. Chem.* **1998**, *12* (10/11), 707–713.
(43) Kim, G. M.; Qin, H.; Fang, X.; Sun, F. C.; Mather, P. T. *J. Polym. Sci., Part B: Polym. Phys.* **2003**, *41* (24), 3299–3313.

(44) Chen, Q.; Xu, R.; Zhang, J.; Yu, D. *Macromol. Rapid Commun.* **2005**, *26* (23), 1878–1882.
(45) Cho, H.; Liang, K.; Chatterjee, S.; Pittman, C. U., Jr. *J. Inorg. Organomet. Polym.* **2006**, *15* (4), 541–553.
(46) Liu, Y.; Zeng, K.; Zheng, S. *React. Funct. Polym.* **2007**, *67* (7), 627–635.
(47) Kannan, R. Y.; Salacinski, H. J.; Odlyha, M.; Butler, P. E.; Seifalian, A. M. *Biomaterials* **2006**, *27* (9), 1971–9.
(48) Mather, P. T.; Jeon, H. G.; Romo-Uribe, A. *Macromolecules* **1999**, *32*, 1194–1203.
(49) Zhang, W.; Fu, B. X.; Seo, Y.; Schrag, E.; Hsiao, B. S.; Mather, P. T.; Yang, N.-L.; Xu, D.; Ade, H.; Rafailovich, M.; Sokolov, J. *Macromolecules* **2002**, *35*, 8029–8038.
(50) Mather, P. T.; Kim, B.-S.; Ge, Q.; Liu, C. Nonionic telechelic polymers incorporating polyhedral oligosilsesquioxane (POSS) and uses thereof. U.S. Patent 7,067,6060 B2, June 27, 2006.
(51) Lee, W.; Ni, J.; Deng, J.; Kim, B.-S.; Satija, S. K.; Mather, P. T.; Esker, A. R. *Macromolecules* **2006**, *40* (3), 682–688.
(52) Kim, B.-S.; Mather, P. T. *Macromolecules* **2002**, *35*, 8378–8384.
(53) Zheng, L.; Hong, S.; Cardoen, G.; Burgaz, E.; Gido, S.; Coughlin, E. B. *Macromolecules* **2004**, *37* (23), 8606–8611.
(54) Fu, B. X.; Hsiao, B. S.; Pagola, S.; Stephens, P.; White, H.; Rafailovich, M.; Sokolov, J.; Mather, P. T.; Jeon, H. G.; Phillips, S.; Lichtenhan, J.; Schwab, J. *Polymer* **2000**, *42* (2), 599–611.
(55) Fu, B. X.; Hsiao, B. S.; White, H.; Rafailovich, M.; Mather, P. T.; Jeon, H. G.; Phillips, S.; Lichtenhan, J.; Schwab, J. *Polym. Int.* **2000**, *49*, 437–440.
(56) Fu, B. X.; Zhang, W.; Hsiao, B. S.; Rafailovich, M.; Sokolov, J.; Johansson, G.; Sauer, B. B.; Phillips, S.; Balnski, R. *High Perform. Polym.* **2000**, *12* (4), 565–571.
(57) Turri, S.; Levi, M. *Macromolecules* **2005**, *38* (13), 5569–5574.
(58) Mather, P. T.; Qin, H.; Wu, J.; Bobiak, J. Medical Polymers 2006, 5th International Conference Focusing on Polymers Used in the Medical Industry, Cologne, Germany, June 6−7, 2006, 2006, 5/1−5/9.
(59) Mather, P. T.; Liu, C.; Ge, Q. Shape memory polymers based on semicrystalline thermoplastic polyurethanes bearing nanostructured silsesquioxane hard segments. U.S. Patent 2005111388, 2005245719, 20050421, 2005.
(60) Sahatjian, R. A.; Tan, F.; Mather, P. T.; Liu, C.; Campo, C. J. Implantable medical devices comprising polymeric components. U.S. Patent 200535444 2006041767, 20051005, 2006.
(61) Kissel, T.; Li, Y.; Unger, F. *Adv. Drug Delivery Rev.* **2002**, *54* (1), 99–134.
(62) Kubies, D.; Rypacek, F.; Kovarova, J.; Lednicky, F. *Biomaterials* **2000**, *21* (5), 529–36.
(63) Pannu, R. K.; Tanodekaew, S.; Li, W.; Collett, J. H.; Attwood, D.; Booth, C. *Biomaterials* **1999**, *20* (15), 1381–1387.
(64) *Polymer Data Handbook*; Oxford University Press, Inc: New York, 1999.
(65) Chiu, F.-C.; Min, K. *Polym. Int.* **2000**, *49* (2), 223–234.
(66) Kalogeras, I. M.; Stathopoulos, A.; Vassilikou-Dova, A.; Brostow, W. *J. Phys. Chem. B* **2007**, *111*, 2774–2782.
(67) Korley, L. T. J.; Pate, B. D.; Thomas, E. L.; Hammond, P. T. *Polymer* **2006**, *47* (9), 3073–3082.
(68) Waddon, A. J.; Coughlin, E. B. *Chem. Mater.* **2003**, *15* (24), 4555–4561.

BM8004935